ELSEVIER

J. Environ. Radioactivity, Vol. 38, No. 1, pp. 17–46, 1998

PII: S0265-931X(97)00019-2 0265-931X/98 $19.00 + 0.00

The Behavior of Radionuclides in the Soils of Rocky Flats, Colorado

M. I. Litaor[a], G. Barth[b], E. M. Zika[b], G. Litus[b], J. Moffitt[b] & H. Daniels[b]

[a]Tel-Hai Rodman College: Upper Galilee, 12210 Israel
[b]University of Colorado Department of Civil and Environmental Engineering, Boulder, CO 80409-0428, USA

(Received 5 August 1996; accepted 6 February 1997)

ABSTRACT

Radionuclide contamination of soils in Rocky Flats, Colorado, resulted from leaking drums of Pu-contaminated oil stored at an outdoor area. To evaluate the mechanisms of radionuclide transport from the contaminated soils to groundwater, an advanced monitoring system was installed across a toposequence. The impact of natural rain, snowmelt, and large-scale rain simulations on the mobility and distribution of the radionuclides in soil interstitial water was studied. The distribution of radionuclides during the monitoring period from 1993 to 1995 suggested that Pu-239 + 240 and Am-241 are largely immobile in semi-arid soils. Large-scale rain simulations with a 100-year recurrence interval occasionally remobilized large fluxes of radionuclides that constitute between 1 and 3·3% of the stored Pu and Am in these soils. Fractionation of Pu-239 + 240 and Am-241 to different particle sizes in the soil interstitial water suggested that most of the radionuclides (83–97%) were associated with suspended particles, whereas the level of radionuclides associated with colloidal (0·45 μm > X > 1 nm) and nonfilterable (< 1 nm) fractions ranged from 1·5 to 15%. © 1997 Elsevier Science Ltd

INTRODUCTION

The potential for mobilization of radionuclides from contaminated soils to groundwater is poorly understood. Early studies suggested that Pu is

largely immobile in the soil environs (Little and Whicker, 1978; Little *et al.*, 1980). However, Hakonson *et al.* (1981) asserted that leaching of soluble Pu through the soil is probably an important process. Penrose *et al.* (1990) found that Pu and Am were transported in groundwater for at least 3·4 km down gradient from the point of discharge. These actinides were tightly or irreversibly bound to colloidal material (25–450 nm). Litaor *et al.* (1994) found evidence that small amounts of radionuclides move down the soil column through a network of macropores formed by decayed root channels and other biological processes. Indeed, groundwater samples collected from a well located 10 m downhill from soils exhibiting an extensive network of macropores showed occasionally elevated activities of Pu-239 + 240 (maximum observed activity of 0·85 Bq l^{-1}). To assess the physicochemical conditions in which Pu-239 + 240 and Am-241 may be transported to groundwater, Litaor *et al.* (1996) conducted small-scale (6 m^2) rain simulations and found that under the experimental conditions, most of the movement of radionuclides was restricted to the top 20 cm of the soil profile. A transport mechanism involving discrete Pu-oxide particles, coupled with macropore channeling, was proposed to explain the observed activities of radionuclides in the soil.

To ascertain further the mechanisms that may mobilize radionuclides from surface soil to groundwater, an extensive monitoring program was conducted. The activities of radionuclides in the soil interstitial water was determined, following natural precipitation events and large-scale (180 m^2) rain simulations. The monitoring program was conducted over 3 years, during which the precipitation varied widely in depth and intensity. The specific objectives of the study were:

(1) to study the impact of snowmelt and natural rainfall on the edaphic factors that control the movement of Pu-239 + 240 and Am-241 from the contaminated soil to groundwater,
(2) to ascertain the mobility of radionuclides in contaminated soil under large scale simulations of extreme rainfall events, and
(3) to evaluate the transport potential of the radionuclides by characterizing the distribution of Pu and Am among particulate, colloidal, and dissolved phases.

Study area

Plutonium contamination of soils at Rocky Flats Plant (Fig. 1), located 25 km northwest of Denver, Colorado, originated primarily from a former storage site where steel drums were used to store plutonium-

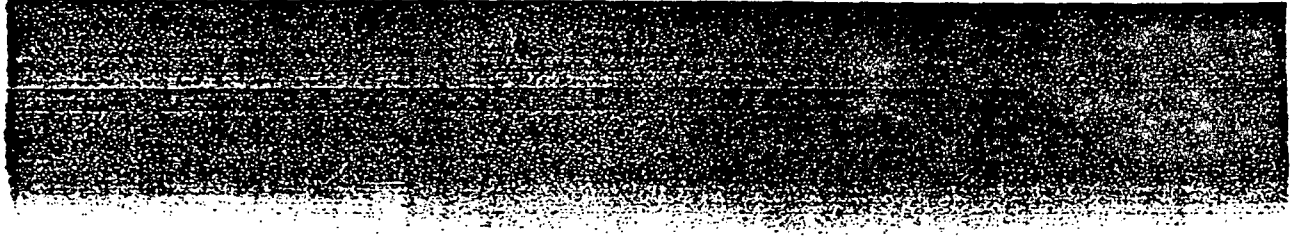

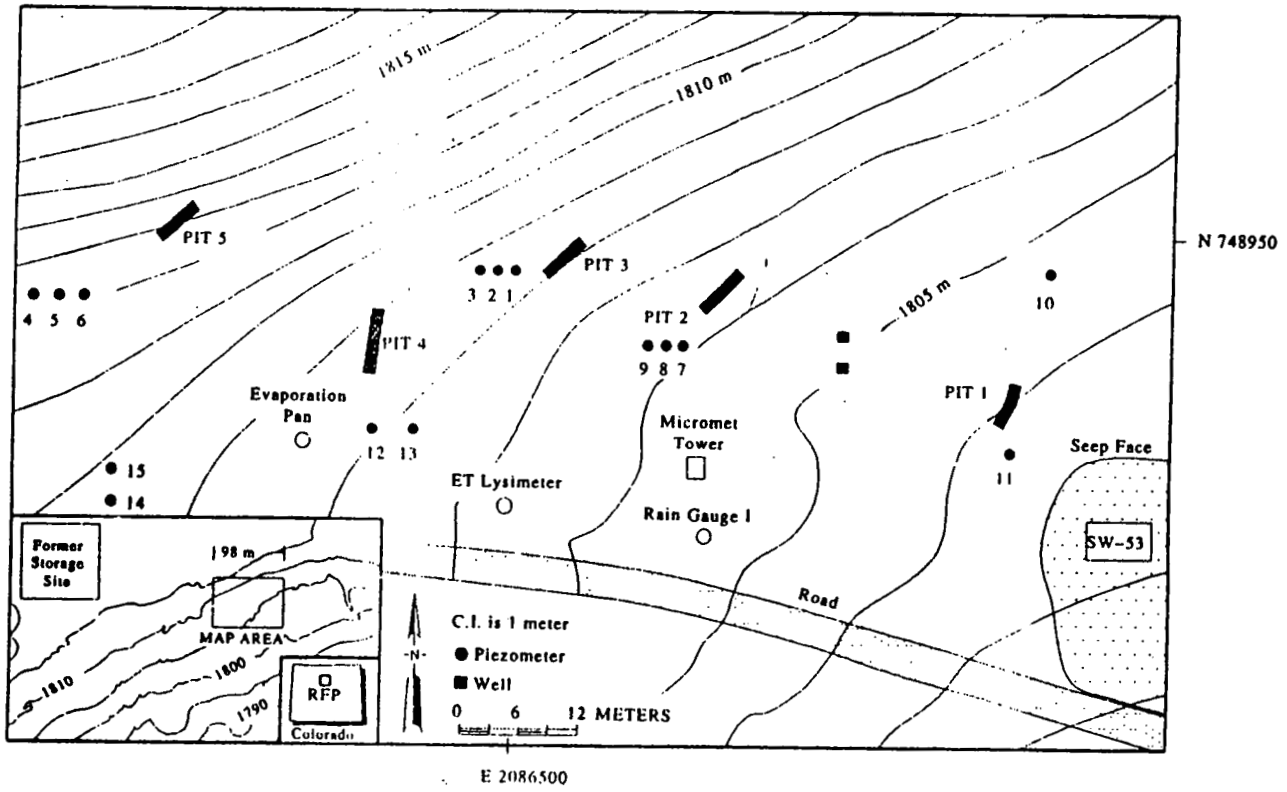

Fig. 1. The location of the instrumented site.

contaminated industrial oils from 1958 to 1968 (Krey and Hardy, 1970; Seed *et al.*, 1971). The average elevation of Rocky Flats is approximately 1810 m, and the the average annual precipitation is 38·7 cm. Rocky Flats is located on broad eastward sloping colluvial deposits of early to late Pleistocene that have been incised in some areas by deep drainage systems. The study site is characterized as a reclaimed mixed grassland transected by wet meadow/marsh ecotone. The dominant species are common mullien (*Verbascum thapsus* L.), Kentucky bluegrass (*Poa pratensis.* L), Japanese brome (*Bromus japonicus Thumb. ex Murr*), prickly lettuce (*Lactuca serriola* L.), Canada thistle (*Cirsium arvense*). Baltic rush (*Juncus balticus Willd.*), western wheatgrass (*Agropyron Smithii Rydb.*), alyssum (*Alyssum minus*), and Cheatgrass (*Bromus tectorum* L.). The mean foliar cover is approximately 90%, whereas the ground cover is 80% litter, 19·8% vegetation, and 0·2% rock.

METHODS

Soil sampling

In 1992, five soil pits along a contaminated toposequence were excavated and sampled for radionuclide activity, and for physical, chemical, and mineralogical properties [see Litaor *et al.* (1994) for details]. Each pit was approximately 5 m long, 1 m wide, and 1 m deep. Because random sampling within the vadose zone in areas characterized by preferential flow is likely to underestimate contaminant transport (Kung and Donohue, 1991), the number of pits investigated and their exact positions were determined by a ground penetrating radar (GPR) survey that located subsurface lateral discontinuities (Litaor *et al.*, 1994). The lateral discontinuities may facilitate increased transport of actinides because of the preferential pathway. Pits 2–5 were excavated to intersect diagonally the lateral discontinuities. Pit 1 was located approximately 4 m above a spring, locally known as SW-53 (Fig. 1) that receives most of its water from a subcropping sandstone layer located below the toposequence.

To minimize flow interference and convergence into the pits (Atkinson, 1978), each pit was back-filled by hand after the installation of monitoring equipment in the upslope face of the pit. During back-filling, special attention was given to soil placement, in order to prevent flow between the instrumented face and the refilled material. The reconstruction of the pits also paid particular attention to the origin of the spoil material (i.e. the spoil material that originating from the A horizon was placed against the A horizon, etc.).

Monitoring system

The monitoring system (MS) consisted of eight major modules:

(1) automated zero-tension samplers that collected water flowing gravitationally, mainly through macropores;
(2) time-domain reflectometry (TDR) probes, which measured in-situ volumetric water content;
(3) automated piezometer network that monitored groundwater level;
(4) temperature probes;
(5) snowmelt monitoring system;
(6) automated monolithic, weighing evapotranspiration lysimeter and evaporation pans;
(7) micrometeorological tower; and
(8) a telemetry communication network coupled with a graphic user interface (GUI) that processed and archived the data.

Zero-tension samplers

Each zero-tension sampler (ZTS) is a trough designed to collect gravitationally flowing water (Litaor, 1988). A ZTS consisted of a half-section of polyvinylchloride (PVC) pipe (36 cm × 15 cm), capped at one end. The ZTSs were inserted into the soil face using a hydraulic jack in locations where macropores (> 1 mm) were evident. A detailed account of the ZTS installation, semi-automated retrieval system, and its setup is given in Litaor *et al.* (1996).

In general, five ZTS were installed within three soil depth increments for a total of 15 ZTSs per pit (Fig. 2). The sampling depth increments were (in cm): 0–20, 20–40, and 40–70. The exact number of ZTSs and their placement were determined from a visual examination of the location and distribution of macropores, and field assessment of the vertical and lateral heterogeneity of the soil. It was assumed that the gravitationally flowing water collected by the ZTSs represented primarily macropore channeling, with limited additional flow from the soil matrix (Luxmoore, 1991).

Time-domain reflectometry probes

Soil water content was monitored by TDR probes, manufactured by Campbell Scientific Inc. (CSI), Logan, UT, USA. A single probe consisted of two wave guides connected to a parallel transmission cable. The probes were linked to a cable tester (Tektronix 1502B)

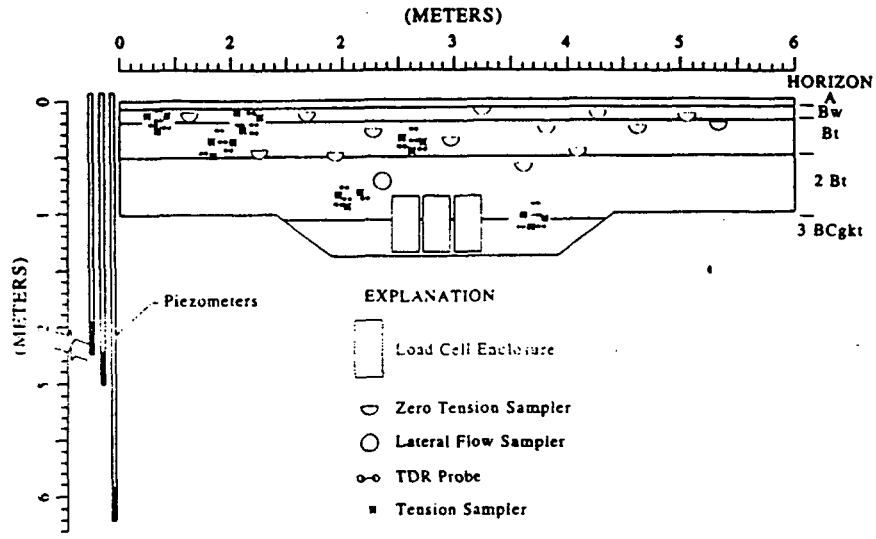

Fig. 2. Schematic diagram of Pit 2. Similar instrumentation was installed in all pits under study.

through a hierarchy of multiplexers. Three tiers of multiplexers were necessary to monitor all the TDR probes. At sampling time, the datalogger activated the appropriate multiplexers, triggered the cable tester, analyzed the cable tester signal and advanced the multiplexer, repeating the process until 120 TDR probes had been sampled. A balance transformer was used to match the impedance of the parallel transmission cables to the 50Ω coaxial cable that connected the cable tester with the multiplexers. The CSI datalogger used the Ledieu *et al.* (1986) algorithm to convert the transit time of the electromagnetic pulse along a probe into volumetric soil moisture content.

In each pit, probes were inserted in clusters of four, with two clusters per depth at three different depths for a total of 24 probes per pit (Fig. 2). Each set of four probes was clustered with three tension samplers. The parallel wave guides were placed horizontally into a soil horizon. The number and locations of TDR probes were determined from field observations of lateral and vertical heterogeneity of the soils.

Piezometers

During the summer of 1994, a network of 15 piezometers was installed in clusters ranging from one to three (Fig. 1). A pressure transducer was placed inside the piezometers (2·54 cm) to measure the piezometeric

surface automatically. The Keller-PSI model no. 169-110-0010 pressure transducer was used in a 0–6·9-kPa range to accommodate the depth of the piezometers ranging from 2·4 to 9 m. Data from the piezometers were queried every 90 min.

Micrometeorological monitoring

To quantify the water equivalent produced from snowmelt, a detailed energy balance study was conducted (Moffitt, 1996). The snow monitoring system consisted of a micrometeorological tower and four pit-based snow stations. The 5-m meteorological tower was installed at the center of the Site (Fig. 1) to measure short- and long-wave radiation, wind, air temperature, and vapor pressure profiles. Radiation components were measured using two pyranometers, one for incoming and the other for reflected short-wave solar radiation, a pyrgeometer measuring incoming long-wave radiation, and a net radiometer. Wind speeds were collected at heights of 0·5, 2·0 and 5·0 m. Relative humidity and atmospheric temperature were measured at 0·5, 2·0 and 4·4 m. The snow stations consisted of snowmelt pans (1 m^2 collection pan draining into a subsurface rain gauge), sonar snow depth sensors, wind speed and direction at 2 m, atmospheric temperature at 2 m, an array of adjustable temperature probes to measure the snowpack temperature profile (at default heights of 0, 2·5, 5, 7·5, 10, 12·5 and 15 cm), and two additional soil temperature probes at 10 and 20 cm below the ground surface.

A Texas Instruments TE525 tipping bucket rain gage recorded precipitation at the site every 5 min. The gage, located centrally in an open area protected by an Alter-Type Wind Screen, continually recorded the natural precipitation reaching the site in 0·025-cm increments.

Evapotranspiration studies

Evapotranspiration (ET) rates and their impact on recharge at the site were studied using an automated evaporation pan, an automated monolithic, weighing evapotranspiration lysimeter and a micromet station (Daniels, 1996). The evaporation pan was used to determine the rate of evaporation from a free water surface and provided information on potential ET. The ET lysimeter measured actual evapotranspiration, interception, and infiltration rates under field conditions. To ensure that the ET lysimeter represented the study site, a network of TDR and soil temperature probes was installed in the lysimeter and the adjacent soil matrix. The micromet station was used

to determine actual and potential ET, using mass- and energy-balance equations (Daniels, 1996).

Graphical user interface (GUI)

The monitoring system consisted of more than 400 sensors clustered in five separate field networks, which performed 60 readings at 10-min intervals, 25 readings at 15-min intervals, and over 300 readings at 90-min intervals. The MS collected more than 3 megabytes of raw data per month. Manual data collection would have been extremely laborious, slow, and prone to user error, thereby impacting data quality and control. Hence, a GUI was developed to automate data retrieval, archiving, and processing. The GUI provided access to a hierarchy of automated functions, including radio communications, system backup, data extraction, plotting and format conversion.

Monitoring program and experimental design of rain simulations

The monitoring period began in January 1993 and was terminated in the spring of 1995 because of the major budget reduction across the DOE complex. All the major snowmelt and natural rain events that produced measurable flow in the soil are summarized in Table 1.

TABLE 1
Natural Rain and Measured Snowmelt Across the Study Area

Natural rain dates	*Total precipitation (cm)*	*Maximum intensity (cm min^{-1})*
06/17–06/18/93	3·86	0·05
04/25–05/2/94	3·37	0·02
06/1–06/20/94	1·54	0·08
08/10–08/11/94	2·48	0·09
05/16–05/18/95	7·92	0·04
Snowmelt dates	*Water equivalent (cm)*	
12/20/93	0·9	
01/26–01/28/94	2·62	
02/11–02/28/94	4·19	
03/26–03/28/94	4·9	
04/4–04/9/94	3·48	
04/27/94	2·68	
11/3–11/13/94	4·9	
02/13/95	3·25	
03/6–03/26/95	3·5	
04/10–04/25/95	7·43	

Rain simulations were also conducted to test the notion that Pu-239+240 and Am-241 in the soils of the site are largely immobile. During the 1993 simulations, the rain simulator wetted an area of ~6 m^2 immediately upslope from the instrumented pits (Litaor *et al.*, 1996). In the 1994 study, a rotating-boom rain simulator mounted on a trailer, with ten arms that extended 7·6 m from a central rotating stem, was used. Each arm had three nozzles that sprayed downward from an average height of 2·4 m. The spatial distribution of rainfall over the wetted area (~180 m^2) had a coefficient of variation of less than 10 percent (Nyhan and Lane, 1986). The rain simulator produced drop-size distributions, impact velocities, and drop sizes similar to natural rainfall (Swanson, 1979), which, in turn, increased the kinetic energy imparted to the ground surface, and increased the recharge rates.

The sequence of simulations followed the procedure established by the USDA and followed by Nyhan and Lane (1985) and Simanton *et al.* (1985) for erosion studies of semi-arid and arid sites. The procedure called for a series of three simulations termed 'dry', 'wet', and 'very wet', which are loosely associated with antecedent soil moisture conditions. The frequency, intensity, and location of the rain simulations are summarized in Table 2. The simulations of constant intensity were performed at an interval of 24 h between the dry and wet runs, and approximately 2 h between the wet and the very wet runs. This series of runs was designed to create a saturated steady-state condition during the wet run, and achieving constant infiltration and runoff rates during the very wet run (Zika, 1996).

During the 1993 experiments, we simulated rainfall of various year-

TABLE 2
Location and Sequence of Rain Simulation Characterized by Intensity of 6 cm h^{-1}

Date	*Time*	*Pit*	*Condition*	*Duration (min)*
6/30/94	8·05	2	Dry	55
7/1/94	10·42	2	Wet	55
7/1/94	13·00	2	Very wet	55
7/7/94	7·30	2	Dry	60
7/8/94	10·00	2	Wet	60
7/8/94	12·00	2	Very wet	60
7/18/94	7·50	2	Dry	60
7/19/94	7·28	2	Wet	60
7/19/94	10·28	2	Very wet	60
11/7/94	15·13	3	Dry	60
11/10/94	14·55	3	Wet	30
11/11/94	13·47	3	Very wet	60

return periods (Litaor *et al.*, 1996). In the 1994 study, only rainfall events with a recurrence of 100-year were simulated to maximize recharge and runoff rates.

Laboratory analysis

The soil interstitial water collected from each ZTS was measured to the nearest 1 ml using a graduated cylinder and briefly described for appearance (i.e. color, clarity, sediment content, and biota, i.e. earthworms). Specific conductance, temperature, pH, and alkalinity were measured in the field, following approved standard operating procedures (EG&G, 1991). The sample turbidity was determined using a Hach Ratio/XR turbidity meter equipped with a 13-mm test tube adapter. The turbidity of the sample was measured on a 0–2000 NTU scale. Samples that exceeded 2000 NTU were reported as > 2000 NTU.

The Pu-239 + 240 and Am-241 activities in unfiltered samples of the soil interstitial water were measured by alpha spectrometry in a commercial laboratory. Samples exhibiting biological components were ashed in an oven at 425–450°C for 8 h. The residue was transfer to a Teflon beaker and was completely dissolved by repeated treatment of HF, 8N HNO_3, and saturated H_3BO_3. Once the solution was clear, it was then passed through an anion exchange column to separate the Pu from the solution (Talvitie, 1971). The Pu was eluted from the column with HCl–NH_4I solution, acidified with HNO_3, and heated to dryness. The sample was redissolved and electroplated on to stainless steel discs. Upon completion of the electroplating, NH_4OH was added to the solution to prevent redissolution of the deposit.

To isolate the Am-241 from the soil interstitial water, the sample was leached with HNO_3. Hydroxides and carbonate-forming elements (e.g. Am) were precipitated out of the leachate with NH_4OH and $(NH4)_2CO_3$, respectively. After drying, the precipitate was redissolved with nitric acid and passed through an anion-exchange column to remove the non-trivalent actinides. Trivalent actinides and lanthanides were co-precipitated with Ca using oxalic acid, Ca carrier, and NH_4OH. The precipitate was redissolved with HCl and passed through a column of mixed anion–cation resin to remove some of the Ca and all of the Fe. Cesium and the remainder of the Ca were extracted from the solution using double extraction into dibutyl-*N,N*-diethycarbamylphosphonate, a back extraction into dilute HNO_3, and then heating to dryness. The sample was redissolved in a dilute-acid solution and passed through an anion-exchange column to remove trivalent lanthanides. This column was washed with a mixture of alcohol, dilute acids, and NH_4SCN for

partial separation of Am from Cm. The sample was then converted to a sulfate form and heated to dryness. Following this, the sample was redissolved and electroplated on to stainless-steel discs. Upon completion of the electroplating, NH_4OH was added to the solution to prevent redissolution of the deposit.

Fractionation of Pu in soil interstitial water

Fractionation of radionuclides into suspended particles ($x > 0{\cdot}45\,\mu m$), colloidal ($0{\cdot}45\,\mu m > x > 10\,kDa$), and dissolved ($< 10\,kDa$) was determined using a fractionation scheme involving ultrafiltration and tangential flow filtration (Buffle and van Leeuwen, 1993; Harnish *et al.*, 1994). Particles larger than $5\,\mu m$ were separated from solution using the Amicon TCF-10, thin-channel ultrafiltration system. This system consisted of a peristaltic pump that circulated the solution through a spiral thin-channel, producing laminar flow over the PCTE 90-mm diameter 5-μm membrane. Subsequent fractionations were achieved with the Minitan ultrafiltration system of Millipore Corp., Bedford, MA, USA. The Minitan tangential flow filtration operates by pumping solution tangentially across a membrane. Particles and molecules smaller than the membrane pores are forced through the membrane by the pressure inside the manifold and are collected as filtrate. Particles and molecules larger than the membrane pores are swept across the membrane and return to the feed reservoir as retentate. The Minitan system separated the sample into three size fractions: (i) $5\,\mu m \geq x \geq 0{\cdot}45\,\mu m$, (ii) $0{\cdot}45\,\mu m \geq x \geq 10\,kDa$, and (iii) $x < 10\,kDa$. To achieve this particle size separation, the Durapore 45-μm and PT series 10-kDa membrane plates were used. The entire tangential flow filtration process was conducted under a nitrogen atmosphere to prevent exposure to ambient air and minimize significant changes in the pH and redox potential of the soil solution.

The above fractionation scheme, as well as the correction protocol for contribution of lesser fractions, was adapted from Harnish *et al.* (1994). One important modfication was introduced, however. Each fraction was corrected for the contribution from all smaller fractions, whereas the correction of Harnish *et al.* (1994) included only the $< 10\,kDa$ fraction. The magnitude of the correction for contribution of lesser fractions varied between 0·0 and 10%.

Soil properties

Particle-size distribution was determined by the pipette method (Soil Conservation Service, 1982). Soil bulk density was measured using the clod method described by Blake and Hartge (1986). Cation exchange

capacity (CEC) was determined by saturating with 0·4 M Na acetate-0·1 M NaCl, followed by washing with 60% ethanol, and replacing the index cation by 0·5 M $Mg(NO_3)_2$ (Rhoades, 1982). Organic C content was determined by dichromate oxidation and titration with $FeSO_4$ (Nelson and Sommers, 1982). The $CaCO_3$ content was determined by a modified pressure calcimeter method described by Nelson (1982). Minerals in the clay fractions were identified by standard X-ray diffraction techniques. Semi-quantitative estimates of mineral abundance were made from measuring peak intensities and by comparison with diffractograms of reference clay minerals (Moore *et al.*, 1989).

Data quality

Extremely rigorous quality assurance and quality control protocols were established to meet all the requirements of a waste site characterization study. These practices, approved by State and Federal regulatory agencies, were enforced by an independent party. Duplicate soil solution samples, rinsates, and laboratory duplicate samples were collected throughout the monitoring period. Precision was quantified by calculating the relative percent difference (RPD). A control limit of ±25% for the RPD in laboratory duplicate analysis was recommended by the laboratory data validation guideline drafted by USEPA in 1988. The RPD values for laboratory duplicate samples ranged from 0 to 42·4%, with a mean of 9·3% and a standard deviation of 8·9% for 51 laboratory duplicates. The RPD values for field duplicate samples ranged from 3·0 to 140% with a mean of 26·8% and standard deviation of 32·8% for 35 field duplicate samples. The larger RPD values observed in field duplicate samples compared with laboratory duplicate samples are expected, due to the discrete particle mechanism that controls Pu fate and transport in soil interstitial water (Litaor *et al.*, 1996). The lack of reproducibility in Pu analyses of soil samples contaminated with Pu oxides is well documented (e.g. Sill, 1971).

Statistical analysis

Comparisons of radionuclide activities, chemical concentrations, and volume flux following the rain simulations were conducted using nonparameteric techniques (Norusis, 1994). The mean rank of the Kruskal–Wallis Test and Kolmogrov–Smirnov test provided a measure of similarity between the data sets, where the smallest datum was assigned the rank 1, and the largest datum in a data set was assigned the rank m before the appropriate statistic was computed [see Gilbert (1987), pp. 248–252].

RESULTS AND DISCUSSION

General characteristics

Most of the soils were characterized by relatively large amounts of organic C in the A horizons and moderate CEC throughout the soil profiles (Table 3). Pit 1 located at the toeslope position (Fig. 1), approximately 1 m above groundwater, was classified as fine-loamy, mixed (calcareous), mesic Cumulic Haplustoll. Pits 2–4, located along a colluvial footslope position, exhibited variable depth to groundwater (1·5–2·5 m), and were classified as fine-loamy, mixed, mesic Aridic Argiustoll. Pit 5, located at a steep backslope position approximately 6 m above groundwater, was classified as loamy-skeletal, mixed mesic Aridic Argiustoll. Pit 1 showed the least amount of organic C content, and little increase of clay content with depth, but a significant accumulation of $CaCO_3$ below 27 cm. Pits 2–5 exhibited argillic horizons, with a considerable increase of clay content with depth. The pH of the soils varied between 6·5 and 8·0, with a mean of 7·3±0·5.

Alkalinity, pH, and specific conductance measured in the soil interstitial water collected over the entire monitoring period, across the slope, exhibited a significant increase downgradient, except at Pit 5 (Table 4). Seasonal fluctuation of groundwater elevation across the toposequence occasionally linked the lower horizons of Pit 1 through 4, and may have even reached the surface. This hydrologic interconnectedness of soils across the toposequence is probably the main reason for the observed trend. The increase of CO_2 in the partially saturated soils increased the pH, alkalinity, and electrolytes in soil interstitial water and the $CaCO_3$ content in soils closer to groundwater (i.e. Pit 1). Because Pit 5 is located well above the seasonal fluctuation of the groundwater, its hydrochemistry is somewhat decoupled from the catenary relationships across the toposequence.

Radionuclides distribution in the soil

Plutonium-239 + 240 activity in the top sampling layer (0–20 cm) ranged from 2220 to 11 460 Bq kg^{-1}, with a mean activity of 7250 Bq kg^{-1}, whereas Am-241 activity in the top sampling layer ranged from 1840 to 8840 Bq kg^{-1}, with a mean activity of 5480 Bq kg^{-1} (Table 5). The distribution of Pu-239 + 240 and Am-241 activity in the top 1 m of the soil showed that over 90% of these radionuclides were residing in the upper 20 cm of the soil, except for pit 5, where significant vertical translocation of Pu-239 + 240 and Am-241 was observed (Table 5). The

TABLE 3
Major Physical and Mineralogical Properties of the Five Soils Under Study

Horizon	*Depth (cm)*	*Sand*	*Silt (%)*	*Clay*	*> 2 mm*	*Bulk density ($g\,cm^{-3}$)*	*CEC ($cmol\,kg^{-1}$)*	*Organic C ($g\,kg^{-1}$)*	*$CaCO_3$ ($g\,kg^{-1}$)*	*pH*	*Smectite[a] content (%)*
Pit 1											
A	0–16	46·9	19	34·1	< 5	1·22	28·6	41	20	7·4	5–30
AB	16–27	27·5	31·8	40·7	< 5	1·53	30·3	28	56	7·7	30–60
Bk1	27–58	35·3	29·4	35·3	10	1·43	29·9	13	122	8·0	30–60
Bkg	58–76	35·6	31·3	33·1	20	1·42	25·8	16	107	7·9	30–60
Bg	76–103	41·3	29·5	29·2	30	1·56	22·5	4	90	7·9	> 60
2BCg	103 +	34·2	34·1	31·7	50 +	1·61	24·4	2	56	8·0	> 60
Pit 2											
A	0–7	64·4	19·1	16·5	5	1·01	27·4	104	4	7·2	5–30
Bw	7–19	69·8	15·3	14·9	35	1·39	19·8	54	3	7·0	5–30
Bt	19–50	49·1	16·7	34·2	< 5	1·46	22·8	13	2	7·0	30–60
2Bt	50–105	36·1	27·4	36·5	< 5	1·40	19·8	6	5	7·0	30–60
3BCgk1	105 +	14·1	40·9	45	< 5	1·59	26·5	2	27	7·5	> 60
Pit 3											
A	0–18	67·3	17·1	15·6	10	1·63	27·9	100	10	7·0	5–30
AB	18–35	58·1	15·6	26·3	20	1·36	23·3	20	4	7·1	30–60
Bw	35–51	60·4	13·9	25·7	5	1·48	20·8	9	2	7·0	30–60
BC	51–120	16·0	44·1	39·9	5	1·43	29·6	3	1	7·7	> 60
BCk1	120 +	22·4	43·6	34·0	< 5	1·53	26·0	2	35	7·8	> 60
Pit 4											

14

A	0–18	64·1	18·6	17·3	10	1·09	24·1	160	6	6·7	5–30
Bt1	18–41	38·4	21·6	40·0	20	1·20	27·9	18	4	6·5	5–30
Bt2	41–77	37·9	23·6	38·5	25	1·50	19·7	6	1	7·5	30–60
BCg	77–108	38·6	23·9	37·5	< 5	1·50	26·4	4	9	7·3	> 60
2BCg	108 +	24·4	37·2	38·4	< 5	1·41	26·4	4	4	7·8	> 60
Pi 5											
A	0–15	62·3	22·3	15·4	30	1·15	20·5	69	9	7·6	5–30
Bt	15–48	57·7	20·5	21·8	80	1·27	21·6	44	9	7·6	5–30
Btg	48–120	43·8	25·9	30·3	5	1·82	25·9	7	6	6·0	> 60

[a]Relative abundance of clay size (< 2 μm).

TABLE 4

Comparison Between Mean Values of pH, Alkalinity, and Specific Conductance Using the Mean Rank of the Kruskal–Wallis Test Across the Toposequence

Pit	*pH*	N	*Mean rank*	*Kruskal–Wallis test*	*Alkalinity* ($mg\,l^{-1}$)	N	*Mean rank*	*Kruskal–Wallis test*	*SC* ($dS\,m^{-1}$)	N	*Mean rank*	*Kruskal–Wallis test*
1	7·57	86	594	$\chi^2 = 174$;	104	67	393	$\chi^2 = 71$;	0·60	85	537	$\chi^2 = 115$;
2	6·94	189	350	Prob > $\chi^2 = 0{\cdot}001$	61	150	252	Prob > $\chi^2 = 0{\cdot}001$	0·47	187	383	Prob > $\chi^2 = 0{\cdot}001$
3	6·90	190	329		44	139	228		0·36	189	344	
4	6·65	141	232		41	84	205		0·30	142	297	
5	6·90	95	349		47	77	268		0·24	95	244	

TABLE 5
Plutonium and Americium Activity in the Five Pits Under Study

Depth (cm)	Pu-239 + 240		Am-241	
	$Bq\,kg^{-1}$	%	$Bq\,kg^{-1}$	%
Pit 1				
0–20	2220	96	1840	94
20–40	16	3·5	15	5·5
40–70	3	0·5	0·8	0·5
Pit 2				
0–20	5270	91·3	4030	91·6
20–40	150	8·5	57	8·0
40–70	2	0·2	0·9	0·4
Pit 3				
0–20	6890	96·3	5480	95·5
20–40	99	3·7	42	3·6
40–70	0·6	0·03	5·2	0·9
Pit 4				
0–20	10400	98·3	8840	99·1
20–40	61	1·4	8·4	0·5
40–70	8	0·3	2·1	0·4
Pit 5				
0–20	11460	79·1	7200	75·0
20–40	68	19·7	290	23·5
40–70	38	1·1	12	1·5

coarse texture of Pit 5 (Table 3), typical for its steep location, probably facilitated higher leaching rates than the soils at the lower reaches of the toposequence.

Radionuclide activity in soil solutions collected during the monitoring period exhibited the highest Pu-239 + 240 and Am-241 activity in the top sampling depth of Pit 5 (Fig. 3). Radionuclide activity decreased systematically across the toposequence and with depth of sampling ($F = 45$, $p < 0{\cdot}001$; $F = 140$, $p < 0{\cdot}001$, respectively). The lowest activities

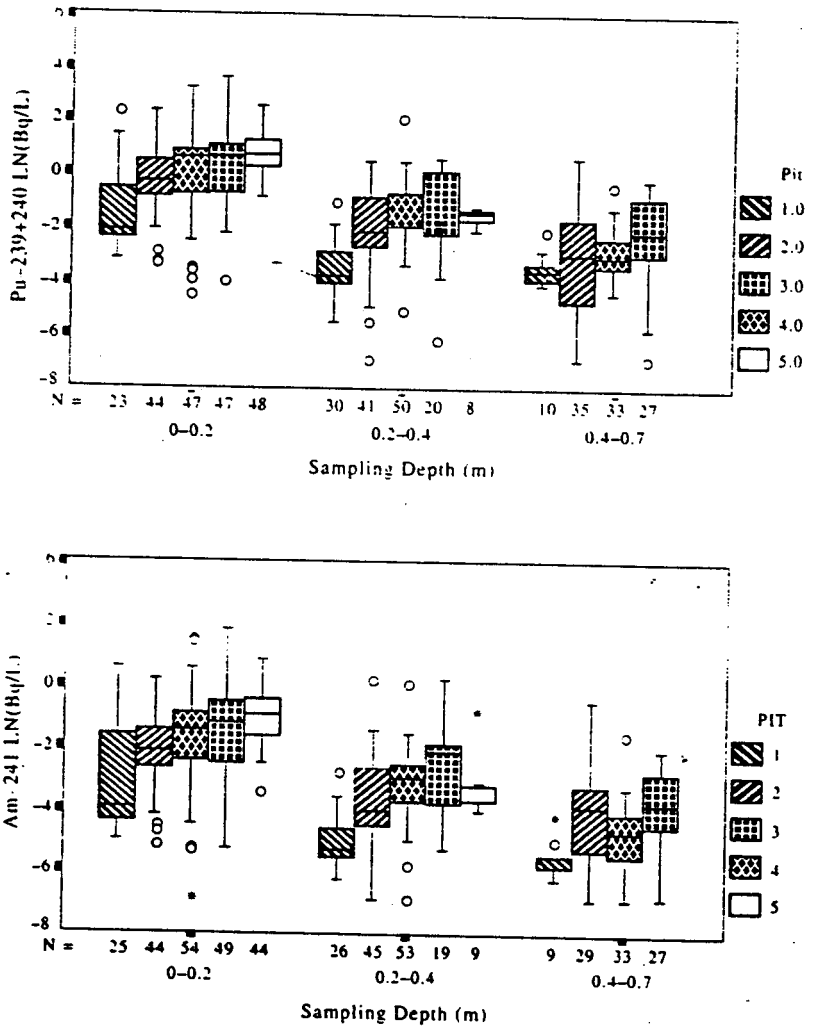

Fig. 3. The distribution of Pu-239 + 240 and Am-241 activities across the toposequence and depths of sampling during the monitoring period.

were observed in Pit 1 at all sampling depths. The mean activity of Pu in the soil interstitial water collected in the top sampling depth was highly correlated with Pu activity in the soil samples (Fig. 4). This correlation exhibited a small standard error and was highly significant ($p < 0.001$). A similar pattern was observed with Am-241 (not shown). The distribution of the radionuclides across the toposequence in soil and interstitial water was diametrically opposed to the distribution of pH, alkalinity, and specific conductance in these soil solutions (see Table 4). This pattern supports the notion that the highly insoluble Pu oxide particles (Martell, 1975) are unaffected by the pH, carbonate complexation, and the ionic strength of the soil solutions observed at the site.

The median Am-241/Pu-239 + 240 activity ratio in the five pits varied between 0·15 in the top soil to 0·2 in the soil samples collected between 0·4 and 0·7 m. The apparent increase in Am/Pu activity ratio with depth was due to a few outliers (Table 6). The Am-241/Pu-239 + 240 activity ratio in the soil interstitial water collected during the monitoring period did not increase significantly with depth (Table 6). These ratios agreed reasonably well with the activity ratio calculated (0·17) and measured (0·19) in soils of the entire site (Litaor, 1995). The results indicated that

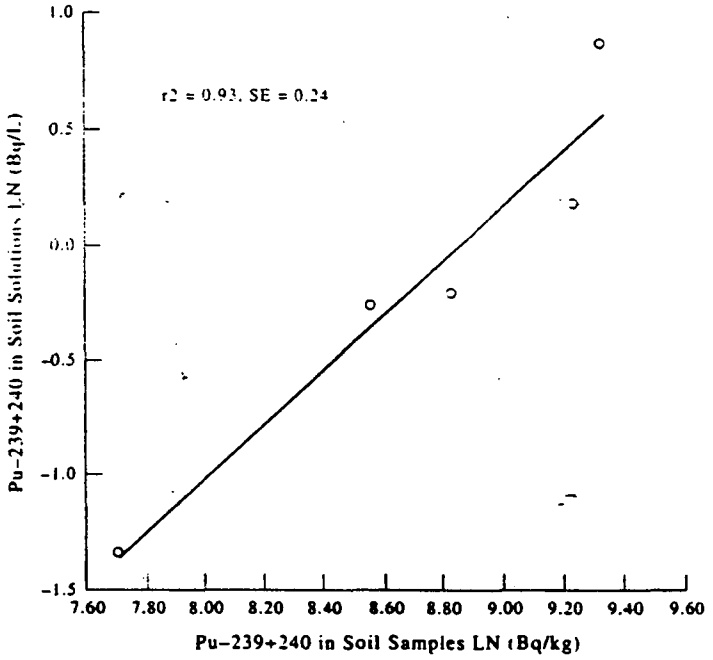

Fig. 4. The relatioship between Pu activity in soil ($Bq\,kg^{-1}$) and the mean activity of Pu-239 + 240 in soil interstitial water ($Bq\,l^{-1}$) collected during the monitoring period.

18

TABLE 6
Am-241/Pu-239+240 Activity Ratio in Soils and Soil Interstitial Water Across the Toposequence

Soil Depth (m)	X	m	*SD*	N
0–0·2	0·16	0·15	0·05	25
0·2–0·4	0·15	0·14	0·06	10
0·4–0·7	0·90	0·20	1·5	10
Soil interstitial water				
	X	m	*SD*	N
0–0·2	0·52	0·18	3·71	200
0·2–0·4	0·23	0·16	0·52	139
0·4–0·7	0·20	0·16	0·20	96

X = arithmetic mean; m = median; SD = standard deviation; N = number of measurements.

Am-241 does not move faster than Pu-239+240 in the soils of Rocky Flats. These findings are in disagreement with the notion advanced by Fowler and Essington (1974) who ascertained that Am-241 is more soluble than Pu-239+240 and may become the radionuclide of prime concern because of a faster migration rate in soils.

Hydrological characterization

The volume flux in all sampling depths was significantly higher during the snowmelt period compared with summer precipitation (Table 7). The volume flux as defined here is the water volume collected by the ZTS divided by the ZTS area (0·054 m^2). These differences probably resulted from higher evapotranspiration rates in the summer (12·7 cm $month^{-1}$) compared with the winter (< 2 cm $month^{-1}$) (Daniels, 1996). The soil temperature below the snow cover was well above freezing and ranged between 2·3 and 8·9°C; thus, no ice layer was formed that may have prevented infiltration. The enhanced volume flux during snowmelt was limited, however, to the first 1 m of the unsaturated soil with no measurable recharge to groundwater (Fig. 5). The soil moisture content in the top sampling depth increased dramatically following the first snowmelt in the fall of 1994 (see Table 1) and remained relatively high during the remainder of the snowmelt season. A similar trend was observed for the deeper sampling intervals; however, the soil moisture content at 40–70 cm rarely increased above 0·25 $m^3 m^{-3}$, which suggested that a limited amount of water reached the lower portion of the soil. Moreover, the piezometric surface continued to decline until the end of April 1995 which suggested that the recharge rate during the snowmelt

TABLE 7

Results from the Two-sample Kolmogorov Smirnov Test Used to Compare the Water and Pu Fluxes Resulting from Rain and Snowmelt Events at Different Depths During the Monitoring Period

Precipitation	*Depth (cm)*	N	*Flux (cm event^{-1})*			*Mean rank*	*Kolmogorov–Smirnov*
			X	m	*SD*		
Rain	0–20	90	0·96	0·58	1·29	53·3	Z = 6·6; Prob < 0·001
Snowmelt		180	10·3	6·6	14·5	176·5	
Rain	20–40	22	0·92	0·47	1·0	47·9	Z = 5·0; Prob < 0·001
Snowmelt		60	6·5	3·7	9·0	124·3	
Rain	40–70	43	0·21	0·04	0·3	22·4	Z = 4·0; Prob < 0·001
Snowmelt		29	4·4	3·4	3·2	57·4	
			Pu-239 + 240 (Bq m^{-2} event^{-1})				
Rain	0–20	35	12·7	4·7	17·1	57·8	Z = 1·2; Prob < 0·09
Snowmelt		95	19·2	8·0	34·7	68·3	
Rain	20–40	20	3·2	1·1	5·0	43·6	Z = 0·6; Prob < 0·8
Snowmelt		45	1·9	0·8	3·5	40·7	
Rain	40–70	35	1·5	0·8	2·2	14·6	Z = 0·27; Prob < 0·8
Snowmelt		25	0·9	0·6	1·0	13·0	

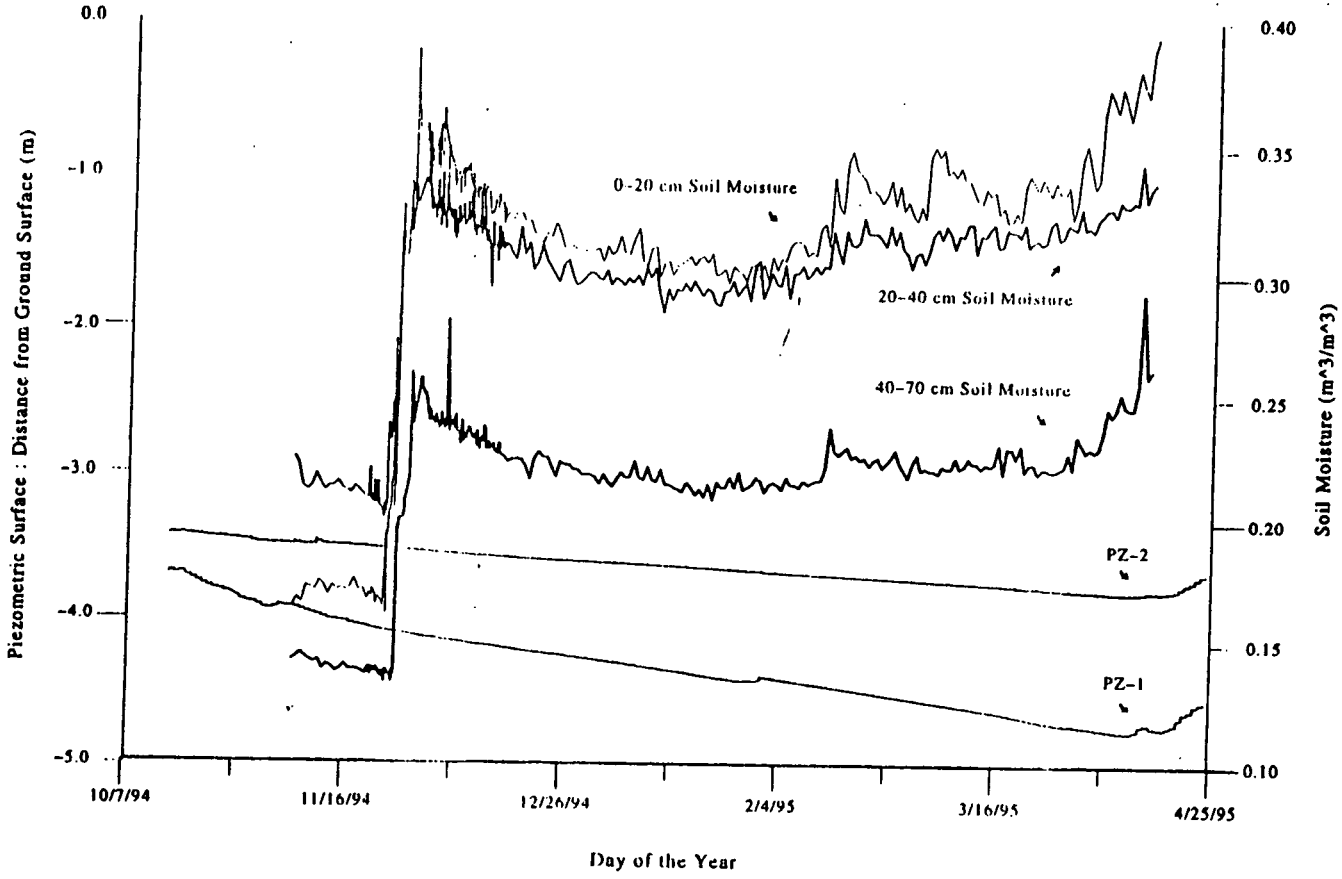

Fig. 5. Soil moisture content and piezometric surface during the snowmelt recorded in 1994 and 1995.

period was insignificant. These results indicate that the potential of radionuclides transport to groundwater from the contaminated soils under the observed hydrological conditions was minimal. It should be noted, however, that the total snow accumulation and its corresponding water equivalent per event during the monitoring period were significantly lower than extreme events recorded in this area. For example, the wettest snowfall on record occurred on 3 April 1986. That event exhibited 0·31 m of total accumulation with a water equivalent of 9·04 cm. This compares with 7·43 cm of water equivalent measured during 15 days in April 1995 (see Table 1). The impact of such snowfall on the hydrological conditions and subsequent radionuclides transport at the Site is currently unknown and could not be resolved by the short monitoring period.

The larger volume flux during the snowmelt season compared with equivalent summer rainfall resulted in higher Pu flux in the top sampling depth during the winter period (Table 7). No significant difference in Pu flux was observed between snowmelt and natural rain at deeper sampling depths, even though the volume flux during the snowmelt at these depths was several orders of magnitude larger than during summer precipitation. This pattern can be explained by the discrete particle phenomenon where translocation of radionuclides to deeper soil horizons may be constrained by macropores too small to accommodate the transport of the discrete particles of Pu oxides (Litaor *et al.*, 1996).

Rain simulations

The vertical distribution of radionuclides in the soil interstitial water suggested that the transport of these contaminants to groundwater following natural rain and snowmelt was minimal. However, none of the recorded snowmelt and natural rain during this period (see Table 1) exceeded a 25-year recurrence interval. Hence, large rain simulations (100-year recurrence interval) were conducted to test further the hypothesis that Pu-239 + 240 and Am-241 in the soils of the site were essentially immobile. The rain simulation sequence did not mobilize the radionuclides down the soil column in large amounts; however, a considerable number of outliers and extreme fluxes were observed during all simulations (Fig. 6). Occasional outliers were even observed in the 40–70-cm sampling depth. These outliers implied that, under the experimental conditions, Pu-239 + 240 and Am-241 may be transported to greater depths than observed during either natural events or the small rain simulations (Litaor *et al.*, 1996). The significant recharge of groundwater that ranged between 9 and 130 cm during the wet rain

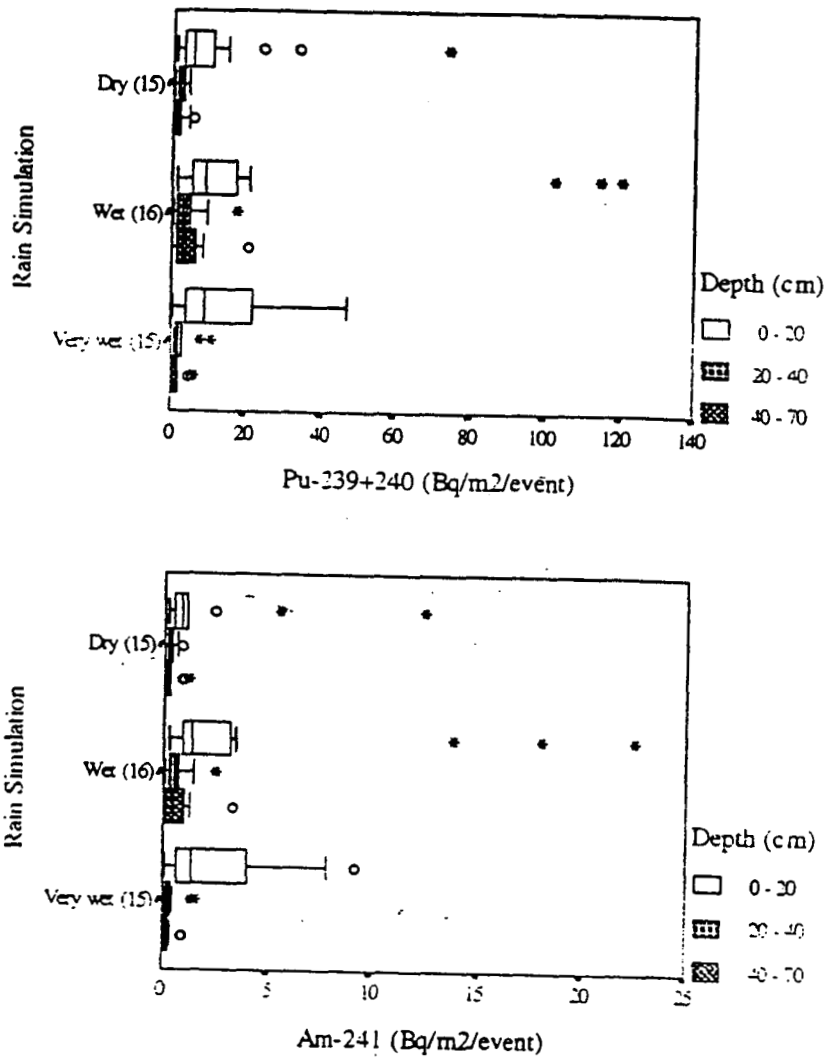

Fig. 6. The vertical distribution of Pu-239 + 240 and Am-241 activity in soil interstitial water following the large-scale rain simulations.

simulations, compared with no measurable recharge during the monitoring period (Fig. 5), suggests that isolated but large rainfall events may be important in translocating radionuclides to groundwater.

To better evaluate the magnitude of the radionuclides translocation during the rain simulations, the observed fluxes were compared with the inventory of Pu-239 + 240 and Am-241 in Pit 2 (Table 8). The inventories of Pu-239 + 240 and Am-241 in Pit 2 were calculated using the weighted mean of the radionuclide activity ($Bq\,kg^{-1}$) times the

TABLE 8
Inventories and Fluxes of Pu-239+240 and Am-241 Following the Rain Simulation in Pit 2

Depth (cm)	Pu-239+240			Am-241		
	$kBq\,m^{-2}$	$Bq\,m^{-2}\,event^{-1}$	%	$kBq\,m^{-2}$	$Bq\,m^{-2}\,event^{-1}$	%
0–20	5270	120	0·002	29·7	22	0·07
20–40	150	17	0·01	2·6	2·4	0·09
40–70	2	20	1·0	0·1	3·3	3·3

weighted mean of the bulk density ($kg\,m^{-3}$, see Table 3) per given sampling depth (m). Using the highest Pu and Am fluxes observed in the top sampling depth, the relative amount of Pu and Am that was remobilized ranged between 0·002 and 0·07% (Table 8). This small amount of remobilization suggested that under experimental conditions, the potential of radionuclides transport from the top soil was insignificant. These results agree well with data gleaned from a sequential extraction experiment (Litaor and Ibrahim, 1996) that clearly demonstrated that under oxic and unsaturated conditions, most of the Pu in the A horizon was strongly adsorbed by organic C and sesquioxides (70–90%).

Flux calculations of Pu and Am in the 40–70-cm sampling depth showed that 1–3·3% of the stored contaminants (Table 8) were translocated to greater depths and, potentially, to groundwater. These results suggest that a large rain event may remobilize Pu-239+240 and Am-241 from the 40–70-cm sampling depth to groundwater, which, in turn, may elevate the radionuclide activity in groundwater to well above the drinking standards of $0{\cdot}002\,Bq\,l^{-1}$. Thus, the occasional elevated Pu activity reported in a shallow well (4·2 m) downslope from Pit 2 as well as seep SW-53 (Fig. 1) can probably be attributed to large rainfalls that produce a wetting front below the top 1 m of the soil.

The Pu flux during the wet simulation was significantly higher than the dry and very wet conditions ($\chi^2 = 12{\cdot}9$; Prob. $< 0{\cdot}001$). Evaluation of the soil moisture data gave some insight into this phenomenon (Fig. 7). Because of the high rates of ET, antecedent soil moisture was similar for both the dry and wet rain simulations. During the wet simulation, the soil probably reached its soil moisture capacity, which ranged from $0{\cdot}35\,m^3\,m^{-3}$ in the top sampling depth to $0{\cdot}45\,m^3\,m^{-3}$ in the 40–70-cm sampling depths. This moisture capacity pattern was consistent with the increase in clay and smectite contents with depths observed in Pit 2 (Table 3). There was no significant difference in soil moisture content measured at the different sampling depths during the 'wet' and 'very wet'

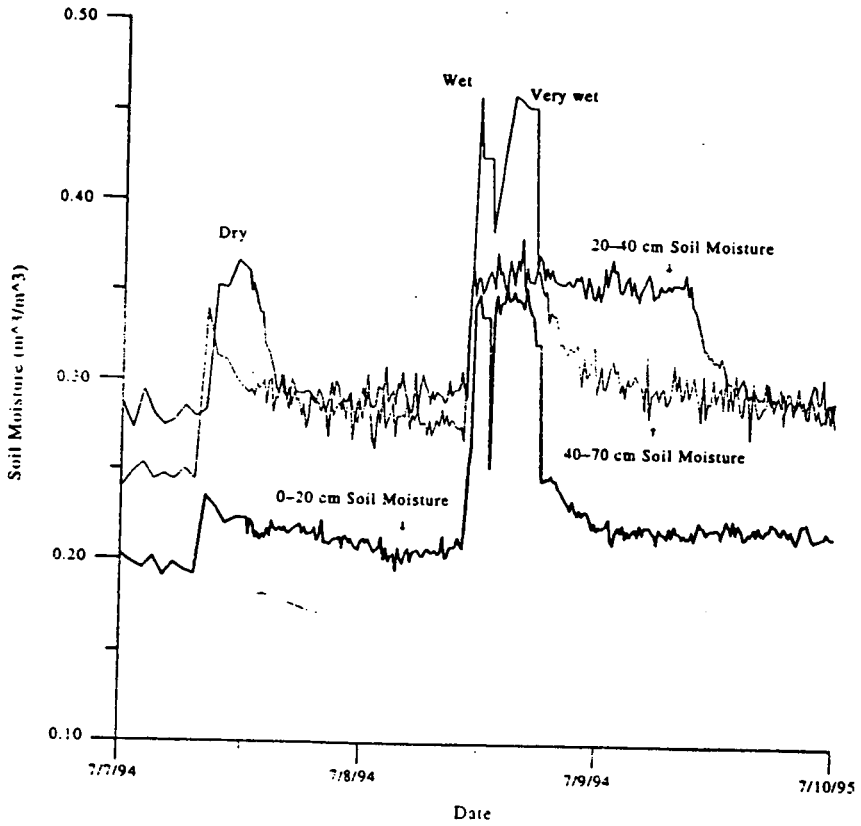

Fig. 7. The soil moisture content profile during a sequence of rain simulation.

conditions. The soil moisture content in the deeper sampling depth decreased rather slowly compared with the top soil. These hydrological conditions facilitated significant runoff rates during the 'very wet' condition ($>0{\cdot}2\,cm\,h^{-1}$ within 10 min from the start of simulation measured at a 35-m^2 plot) compared with the 'wet' condition ($>0{\cdot}2\,cm\,h^{-1}$ only after 60 min of rain simulation) (Zika, 1996). Moreover, the recharge of groundwater during the dry, wet, and very wet simulations averaged 2·7 cm, 63·7 cm, and 34·4 cm, respectively, which clearly demonstrates that the infiltration rate and the potential of radionuclide translocation to groundwater were greatest during the wet simulations.

Fractionation of Pu-239+240 and Am-241 in soil interstitial water

A good correlation was observed among Pu, Am, and turbidity in the soil interstitial water collected during the monitoring period and the rain

TABLE 9
Correlation Matrix Among Pu-239 + 240 ($Bq\,l^{-1}$), Am-241 ($Bq\,l^{-1}$), and Turbidity (NTU)

Depth (cm)		*Am-241*	*Pu-239 + 240*
0–20	Turbidity	0·76	0·77
	Pu-239 + 240	0·95	
20–40			
	Turbidity	0·64	0·65
	Pu-239 + 240	0·84	
40–70			
	Turbidity	0·56	0·57
	Pu-239 + 240	0·96	

simulations in the top sampling depth (Table 9). This correlation suggests that most of the transport of the radionuclides in the top sampling depth was associated with suspended and colloidal matter.

To evaluate this correlation further, seven soil solutions were sampled during the rain simulations and fractionated using ultrafiltration techniques. The activity of radionuclides in the unfiltered samples ranged from 2·4 $Bq\,l^{-1}$ for Pu-239 + 240 and 0·48 $Bq\,l^{-1}$ for Am-241 in the top sampling depth to 0·04 $Bq\,l^{-1}$ for Pu-239 + 240 and 0·009 $Bq\,l^{-1}$ for Am-241 in the deepest sampling depth (Table 10).

The most important finding of the fractionation scheme is the large association of radionuclides with suspended particles (Table 10). Between 83 and 97% of the radionuclides were associated with particles larger than 0·45 μm, regardless of the level of activity and depth of sampling. These results clearly demonstrate the limited mobility of Pu and Am in the soils of the Site since the movement of suspended particles in the soil is highly dependent on the spatial arrangement and continuity of macropores in the soil. A given macropore can be activated during a given event and later may be filled up or truncated, as was demonstrated by Munyankusi *et al.* (1994). Most of the macropores in the top sampling depth were created by earthworm activity (Litaor *et al.*, 1994) or by the dense roots observed in the mollic epipedon across the toposequence. Some macorpores were observed at greater depths (> 150 cm) that were formed primarily by a Canadian thistle (*Cirsium arvense*) and other plants that utilize the shallow groundwater (1–6 m). These macropores may have facilitated the suspended particles transport with depth, as demonstrated in Table 10.

Only minimal activity of radionuclides was associated with the colloidal size fraction (0·3–6·8%); however, a somewhat increased association was detected with filterable (0·6–17·1%) (Table 10). The highest association of nonfilterable Pu and Am was observed in soil interstitial water

TABLE 10
The Fractionation of Pu-239 + 240 and Am-241 in Soil Interstitial Water Collected After Rain Simulations

Pu-239 + 240 *Location and date*	*0–21 cm* *11/11/94*		*0–20 cm* *11/14/94*		*20–40 cm* *11/9/94*		*20–40 cm* *11/14/94*		*20–40 cm* *11/11/94*		*20–40 cm* *11/28/94*		*40–70 cm* *11/14/94*	
	Bq l⁻¹	*%*	*Bq l⁻¹*	*%*	*Bq l⁻¹*	*%*	*Bq l⁻¹*	*%*	*Bq l⁻¹*	*%*	*Bq l⁻¹*	*%*	*Bq l⁻¹*	*%*
$> 5\,\mu m$	1·96	92·7	0·87	90·9	0·33	90·8	0·12	88·6	0·10	82·8	0·11	83·9	0·03	82·9
$5 > x > 0{\cdot}45\,\mu m$	0·09	4·1	0·01	1·3	0·02	6·2	0·0	0·0	0·01	11·2	0·01	8·9	0·0	0·0
$0{\cdot}45\,\mu m > x >$ 10kDa	0·03	1·7	0·05	5·5	0·006	1·5	0·009	6·8	0·003	2·2	0·007	4·9	0·0	0·0
$x <$ 10kDa	0·03	1·5	0·02	2·3	0·006	1·5	0·006	4·6	0·005	3·8	0·003	2·3	0·006	17·1
Am-241														
$> 5\,\mu m$	0·13	89·3	0·33	91·8	0·06	91·0	0·02	91·7	0·02	82·2	0·02	82·6	0·006	93·7
$5 > x > 0{\cdot}45\,\mu m$	0·002	1·2	0·002	5·5	0·005	7·7	0·0	0·0	0·003	9·6	0·003	10·1	0·0	0·0
$0{\cdot}45\,\mu m > x >$ 10kDa	0·007	4·4	0·006	1·7	0·001	0·7	0·0	0·0	0·001	5·5	0·0	0·0	0·0	0·0
$x <$ 10kDa	0·008	5·1	0·004	1·0	0·001	0·6	0·001	6·6	0·001	2·7	0·002	7·3	0·0	6·3

27

collected from the deepest sampling depth (40–70 cm). This pattern may be explained by the increase in clay content, especially Mg-smectite with depth (Table 3), which probably restricted the mobility of suspended particles to only a few large macropores.

The observed increase of Pu and Am in soil interstitial water at all sampling depths following the wet simulations (see Fig. 6 and Table 9) and the observed increase of filterable Pu and Am with depth following these simulations provided an unexpected transport scenario; large rain conditions may transport the radionuclides in suspended and filterable forms from the contaminated soil to groundwater via a few well-developed large macropores. Subsequently, the cumulative increase of filterable Pu and Am with depth may support the transport of radionuclides in groundwater.

The fractionation pattern of Pu and Am in the soil interstitial water provides important information regarding the usefulness of computer models that predict the mobility of radionuclides in the soil environment. Most of these models utilize a distribution coefficient (K_d) to compute the relative velocity of the radionuclides. By using the K_d it is assumed that the reaction is fast, reversible, and linear with respect to the concentration of the sorbed radionuclides in the soil versus the activity of radionuclides in solution. The fractionation results suggest that only a minor component of the radionuclides is in the 'dissolved' form, and the reactivity of this fraction with the soil media is unknown. Hence, the common use of K_d values in predicting the movement of radionuclides in the soil environment is questionable.

REFERENCES

Atkinson, T. C. (1978) Techniques for measuring subsurface flow on hillslopes. In *Hillslope Hydrology*, ed. M. J. Kirkby, pp. 73–120. Wiley, New York.

Blake, G. R. and Hartge, K. H. (1986) Bulk density. In *Methods of Soil Analysis*, ed. A. Klute, Part 1, 2nd edn, pp. 363–375. Agron. Monogr. 9. ASA and SSSA, Madison, WI.

Buffle, J. and van Leeuwen, H. P. (1993) *Environmental Particles. Environmental Analytical and Physical Chemistry Series*, Volume 2. Lewis, Boca Raton, FL.

Daniels, H. (1996) The role of evapotranspiration in the geohydrologic cycle at Rocky Flats. Master thesis, University of Colorado, Boulder, CO.

EG&G (EG&G Rocky Flats, Inc.) (1991). *Environmental Management Department, Volume II, Manual No. 5, 21000-OPS-GW*. Rocky Flats Plant, Golden, CO.

Fowler, E. B. and Essington, E. H. (1974) Soils element activities October 1972–September 1973. In *The Dynamics of Plutonium in Desert Environments*, eds P. B. Dunnaway and M. G. White, pp. 7–16. NVO-142.

28

Gilbert, R. O. (1987) *Statistical Methods for Environmental Pollution Monitoring*. Van Nostrand Reinhold, New York, 320 pp.

Hakonson, T. E., Watters, R. L. and Hanson, W. C. (1981) The transport of plutonium in terrestrial ecosystems. *Health Physics* **40**, 63–69.

Harnish, R. A., McKnight, D. M. and Ranville, J.F. (1994) Particulate, colloidal and dissolved phase associations of plutonium and americium in a water sample from well 1587 at the Rocky Flats Plant, Colorado. US Geological Survey Water Resources Investigation Report 93-4175, Denver, CO. 27 pp.

Krey, P. W. and Hardy, E. P. (1970) Plutonium in soil around the Rocky Flats Plant. HASL-235.

Kung, K.-J.S. and Donohue, S.V. (1991) Improved solute-sampling protocol in a sandy vadose zone using ground-penetrating radar. *Soil Science Society of America Journal* **55**, 1543–1545.

Ledieu, J.Ridder, P.Clerck, P.Sautrebande, S. (1986) A method of measuring soil moisture by time-domain reflectometery. *Journal of Hydrology* **88**, 319–328.

Litaor, M. I. (1988) Review of soil solution samplers. *Water Resources Research* **24**, 727–733.

Litaor, M. I. (1995) Spatial analysis of Pu-239 + 240 and Am-241 in soils around Rocky Flats, Colorado Plant. *Journal of Environmental Quality* **24**, 506–516.

Litaor, M. I., Barth, G. R. and Zika, E. M. (1996) Fate and transport of actinides in the soil of Rocky Flats, Colorado. *Journal of Environmental Quality* **25**, 671–683.

Litaor, M. I. and Ibrahim, S. (1996) Plutonium association with selected solid phases in soils of Rocky Flats, Colorado using sequential extraction technique. *Journal of Environmental Quality*. **25**, 1144–1152.

Litaor, M. I., Thompson, M. L., Barth, G. R., Molzer, P. C. (1994) Plutonium-239 + 240 and Americium-241 in soils east of Rocky Flats, Colorado. *Journal of Environmental Quality* **23**, 1231–1239.

Little, C. A., Whicker, F. W. (1978) Plutonium distribution in Rocky Flats soil. *Health Physics* **34**, 451–457.

Little, C. A., Whicker, F. W., Winsor, T. F. (1980) Plutonium in a grassland ecosystem at Rocky Flats. *Journal of Environmental Quality* **9**, 350–354.

Luxmoore, R. J. (1991) On preferential flow and its measurement. In *Preferential Flow*, eds T. J. Gish and A. Shirmohammadi, pp. 12–22. Proceedings of the National Symposium, 16–17 December 1991, Chicago, IL.

Martell, E. G. (1975) Actinides in the environment and their uptake by man. NCAR-TN STR-110.

Moffitt, J. A. (1996) Monitoring and modeling of snowmelt at Rocky Flats. Master thesis, University of Colorado.

Moore, D. M. and Reynolds, R. C. Jr (1989) *X-ray Diffraction and the Identification and Analysis of Clay Minerals*. Oxford University Press, New York.

Munyankusi, E., Gupta, S. C., Moncrief, J. F., Berry, E. C. (1994) Earthworm macropores and preferential transport in a long-term manure applied Typic Hapludalf. *Journal of Environmental Quality* **23**, 773–784.

Nelson, R. E. (1982) Carbonate and gypsum. In *Methods of Soil Analysis*, eds A. L. Page *et al.*, Part 2, 2nd edn, pp. 159–164. Agron. Monogr. 9. ASA and SSSA, Madison, WI.

Nelson, D. W. and Sommers, L. E. (1982) Total carbon, organic carbon, and organic matter. *In Methods of Soil Analysis*, eds A. L. Page *et al.*, Part 2. 2nd

edn, pp. 539–577. Agron. Monogr. 9. ASA and SSSA, Madison, WI.
Norusis, M. J. (1994) *SPSS® Base System, Release 6.0 SPSS Inc.*, Chicago IL.
Nyhan, J. W. and Lane, L. J. (1985) Rainfall simulator studies of earth covers used in shallow land burial at Los Alamos, New Mexico. In *Proceedings of Rainfall Simulator Workshop*, US Department of Agriculture, Tucson, AZ.
Nyhan, J. W. and L. J. Lane (1986). *Erosions Control Technology: A User's Guide to the Use of the Universal Loss Equation at Waste Burial Facilities.* Los Alamos National Laboratory, Los Alamos, NM, LA-10262-M.
Penrose, W. R., Polzer, W. L., Essington, E. H. and Nelson, D. N.Orlandini, K. A. (1990) Mobility of plutonium and americium through shallow aquifer in a semiarid region. *Environmental Science Technology* **24**, 228–234.
Rhoades, J. D. (1982) Cation exchange capacity. In *Methods of Soil Analysis*, ed. A. L. Page *et al.*, Part 2, 2nd edn, pp. 149–157. Agron. Monogr. 9. ASA and SSSA, Madison, WI.
Seed, J. R., Calkins, K. W., Illsley, C. T., Miner, F. J. and Owen, J. B. (1971) Committee Evaluation of Pu Levels in Soils within and surrounding USAEC Installation at Rocky Flats, Colorado. DOW Chemical Company, RFP-INV-1.
Sill, C. W. (1971). The particle problem as related to sample inhomogeneity. In *Proceedings of Environmental Plutonium Symposium*, ed. E. C. Fowler, pp. 81–83. Los Almos Scientific Laboratory, Los Alamos, NM.
Simanton, J. R., Johnson, C. W., Nyhan, J. W. and Romney, E. M. (1985) Rainfall simulation on rangeland erosion plots. In *Proceedings of Rainfall Simulator Workshop*, US Department of Agriculture, Tucson, AZ.
Soil Conservation Service (1982) Procedures for collecting soil samples and methods of analysis for soil surveys. Soil Survey Investigation Report 1. US Government Printing Office, Washington, DC.
Swanson, N. P. (1979) Field plot rainfall simulation (rotating-boom rainfall simulator), Lincoln Nebraska. In *Proceedings of Rainfall Simulator Workshop*, US Department of Agriculture, Tucson, AZ. A-106-12W-12.
Talvitie, N. A. (1971) Radiochemical determination of plutonium in environmental and biological samples by ion exchange. *Analytical Chemistry* **43**, 1827–1830.
Zika, E. M. (1996) Characteristics and impacts of the rainfall–runoff relationships on a radionuclides contaminated hillslope. Master thesis, University of Colorado, Boulder, CO.